

Ring Opening of the Cyclobutane in a Thymine Dimer Radical Anion

Chrysostomos Chatgililoglu,^{*,[a]} Maurizio Guerra,^[a] Panagiotis Kaloudis,^[a] Chantal Houée-Lévin,^[b] Jean-Louis Marignier,^[b] Vijay N. Swaminathan,^[c] and Thomas Carell^[c]

Abstract: The reactions of hydrated electrons (e_{aq}^-) with thymine dimer **2** and thymidine have been investigated by radiolytic methods coupled with product studies, and addressed computationally by means of BB1K-HMDFT calculations. Pulse radiolysis revealed that one-electron reduction of the thymine dimer **2** affords the radical anion of thymidine (**5**) with $t_{1/2} < 35$ ns. Indeed, the theoretical study suggests

that radical anion **3**, in which the spin density and charge distribution are located in both thymine rings, undergoes a fast partially ionic splitting of the cyclobutane with a half-life of a few ps.

Keywords: density functional calculations • radical reactions • reaction mechanisms • thymine dimer • time-resolved spectroscopy

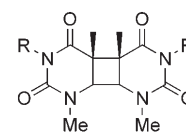
This model fits with the in vivo observation of thymine dimer repair in DNA by photolyase. γ -Radiolysis of thymine dimer **2** demonstrates that the one-electron reduction and the subsequent cleavage of the cyclobutane ring does not proceed by means of a radical chain mechanism, that is, in this model reaction the $T^{\cdot-}$ is unable to transfer an electron to the thymine dimer **2**.

Introduction

Light absorption by DNA in the UVB region results mainly in formation of *cis-syn* cyclobutane thymine dimers ($T < > T$).^[1] Biological repair of these lesions occurs for example by DNA photolyase, which uses light energy to split the $T < > T$ dimer through a radical mechanism.^[2a] The critical repair step is a photoinduced electron transfer from a reduced and light-excited flavin to the thymine dimer which triggers a $[2\pi+2\pi]$ cycloreversion reaction leading to the cleavage of the thymine dimer. By using ultrafast fluorescence spectroscopy, Sancar and co-workers were able to directly observe the electron transfer from the excited flavin

cofactor to the $T < > T$ in 170 ps. Back electron transfer from repaired thymines to the flavin radical occurred inside the protein in 560 ps.^[2b]

Up to now, the mechanism of the splitting of the thymine dimer radical anion has been highly controversial. The knowledge available today on the basic cleavage reaction in solution was mainly gained by the analysis of the N-methylated derivatives **1a** and **1b**. An electrochemical study showed that the radical anion of **1b** is formed prior to two successive homolytic C–C bond cleavage steps.^[3] From the appearance of the monomer radical anion, a rate constant of $1.8 \times 10^6 \text{ s}^{-1}$ for the dimer **1b** radical anion splitting was inferred by using optical measurements at pH 12.^[4] This value is significantly slower compared to the measured value in the enzyme suggesting that the active site stabilizes the transition state enthalpically. Another EPR study suggests, however, that the electron addition to the dimer **1a** followed by ring opening occurs so fast that only the monomer radical anion was detectable at 77 K.^[5] Moreover, **1a** was reported to cleave by a radical chain reaction in one-electron reduction studies,^[6] although the redox potential of **1b** is unfavorable for such a process compared to that of its monomer ($\Delta G \approx +0.1 \text{ eV}$).^[3,7]



1a: R = H
1b: R = Me

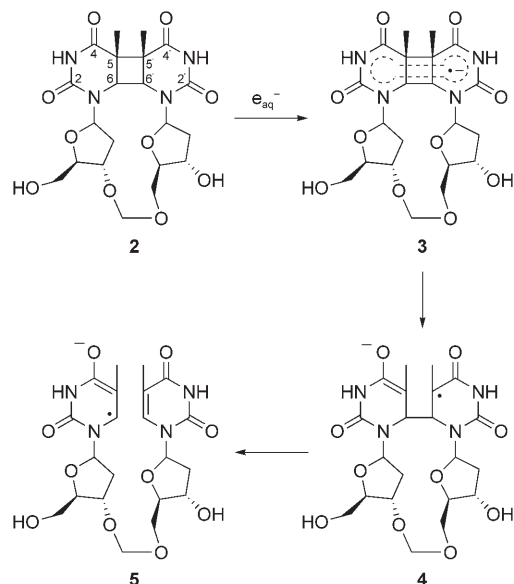
[a] Dr. C. Chatgililoglu, Dr. M. Guerra, P. Kaloudis
ISOF, Consiglio Nazionale delle Ricerche
Via P. Gobetti 101, 40129 Bologna (Italy)
Fax: (+39)051-639-8349
E-mail: chrys@isof.cnr.it

[b] Prof. C. Houée-Lévin, Dr. J.-L. Marignier
Laboratoire de Chimie-Physique
Université Paris-Sud, 91405 Orsay cedex (France)

[c] Dr. V. N. Swaminathan, Prof. T. Carell
Center for Protein Science at the Department of
Chemistry and Biochemistry, LMU Munich
Butenandtstrasse 5–13, 81377 Munich (Germany)

Supporting information for this article is available on the WWW
under <http://www.chemeurj.org/> or from the author.

Cleavage of the thymine dimer in DNA was recently also investigated with model systems because of the large potential of this process for the DNA chip technology.^[8] Particularly the T<>T dimer **2**, which has a CH₂ bridge between the two sugar moieties rather than the normal phosphodiester group (Scheme 1), was prepared in large quantities and

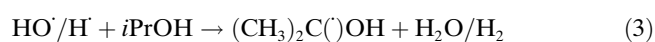
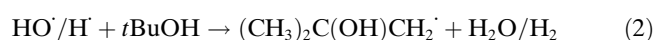
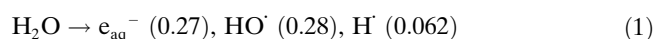


Scheme 1. Proposed mechanism for the reaction of e_{aq}^- with T<>T dimer **2**.

used as a chemical trap for electrons injected into the DNA duplex.^[9] Due to a lack of detailed knowledge about the exact cleavage mechanism of thymine dimers, further use of **2** for a more detailed investigation of the excess electron transfer process had to be postponed.^[10] In order to shed more light on one of Nature's most prominent DNA repair mechanisms, we present herein a chemical radiation and theoretical study on the reaction of hydrated electrons (e_{aq}^-) with T<>T dimer **2** (Scheme 1).

Results and Discussion

Radiolytic production of transients: Radiolysis of neutral water leads to e_{aq}^- , HO \cdot , and H \cdot as shown in Equation (1). The values in parentheses represent the radiation chemical yields (G) in units of μmolJ^{-1} . The reactions of e_{aq}^- with **2** were studied in O₂-free solutions containing 0.2–0.3 M *t*BuOH or *i*PrOH. With this amount of alcohol, most of HO \cdot and H \cdot are scavenged efficiently as shown in Equations (2) or (3).^[11]



Pulse radiolysis studies: The spectral changes obtained from the pulse irradiation of a N₂-purged aqueous solution of **2** (3.4 mM) and *t*BuOH (0.3 M) at pH 8.9 are shown in Figure 1a. The optical absorption spectrum taken 50 ns after the pulse (red) originated from two bands. The band above 350 nm is due to hydrated electrons (e_{aq}^-), whereas the band

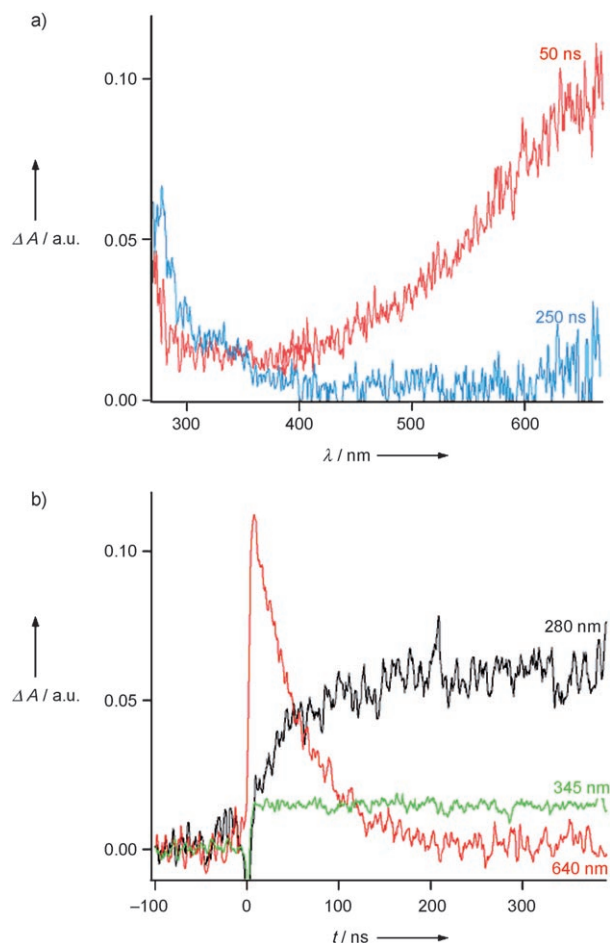


Figure 1. a) Absorption spectra obtained from the pulse radiolysis of Ar-purged solutions containing 3.4 mM **2** and 0.3 M *t*BuOH at pH 8.9 (phosphate buffer 10 mM) taken 50 and 250 ns after the pulse. b) Time dependence of absorption at 640, 345, and 280 nm.

below 350 nm is due to the reaction of **2** with e_{aq}^- . The absorption spectrum taken 250 ns after the pulse (blue) shows the disappearance of e_{aq}^- and the further rise of the transient species due to the reaction of **2** with e_{aq}^- . The pseudo-first-order rate constant for the disappearance of e_{aq}^- was found to be $(1.9 \pm 0.1) \times 10^7 \text{ s}^{-1}$ by measuring the rate of the optical density decrease of e_{aq}^- at 640 nm (Figure 1b, red traces), which corresponds to the bimolecular rate constant of $5.6 \times 10^9 \text{ M}^{-1} \text{ s}^{-1}$ taking into account the nucleoside concentration. In Figure 1b the black traces show the growth of the new transient at 280 nm with kinetics identical to that of e_{aq}^- decay, $k = (2.1 \pm 0.4) \times 10^7 \text{ s}^{-1}$, whereas the green traces at 345 nm correspond to an isobestic point in Figure 1a. It is

also worth mentioning that no spectral change was observed at a longer time scale (up to 1.5 μ s).

The absorption spectrum of the observed transient is very similar in shape and intensity compared to the reported spectrum for the radical anion of thymidine,^[12] that is, the absorptions increase in intensity in going from ≈ 450 to ≈ 300 nm with λ_{max} below 300 nm and a shoulder at ≈ 340 nm. We confirmed this observation by independent experiments obtained after the reduction of thymidine with e_{aq}^- at pH 8.9. The pseudo-first-order rate constant for the disappearance of e_{aq}^- was found to be $(3.5 \pm 0.3) \times 10^7 \text{ s}^{-1}$ by measuring the rate of the optical density decrease of e_{aq}^- at 640 nm (see the Supporting Information), which is two times faster than the reaction with the T<>T dimer **2**. Our findings clearly indicate that the reaction of e_{aq}^- with **2** (the rate-determining step) affords the radical anion **5** and that the ring opening of the intermediate **3** is faster than $2 \times 10^7 \text{ s}^{-1}$ ($t_{1/2} < 35$ ns). This low-limit value is at least one order of magnitude higher than the one reported for the ring opening of the radical anion derived from **1b**.^[4]

DFT calculations: Time-dependent DFT (TD-B3LYP/6-311G**//B1B95/6-31+G**) calculations also suggest that the experimental spectrum can indeed be assigned to the radical anion **5**.^[13] The computed optical transitions for the radical anions **3**, **4** and, **5** in the range of 260–600 nm with an oscillator strength $f > 0.01$ are reported in Table 1. The computed values for **3** are fully inconsistent with the experimental findings, as the two strongest transitions are predicted to occur at 429 and 501 nm. The transition computed at 413 nm for **4** is also absent in the absorption spectrum. On the other hand, the multiple intense transitions between 270 and 290 nm and a shoulder at 364 nm computed for the radical anion **5** strongly resembles the experimental spectrum. The three transitions computed at 270, 276, and 289 nm are excitations of the α -spin electron from the SOMO localized mainly at C6 to the π^* -(C4–C5), σ^* -(N1–C1'), and σ^* -(C1–O) antibonding MOs, respectively, whereas the excitation of the β -spin electron from the HOMO, localized at the π -(C5–C6), to the LUMO localized at C6 is computed to occur at higher wavelengths (364 nm).

Table 1. TD-B3LYP/6-311G**//B1B95/6-31+G** optical transitions (wavelength λ and oscillator strength f) for the radical anions **3**, **4**, and **5**.^[a]

| Radical 3 | | Radical 4 | | Radical 5 | |
|------------------|-------|------------------|-------|------------------|-------|
| λ [nm] | f | λ [nm] | f | λ [nm] | f |
| 268 | 0.018 | 261 | 0.018 | 268 | 0.020 |
| 275 | 0.013 | 316 | 0.014 | 270 | 0.031 |
| 330 | 0.032 | 363 | 0.011 | 276 | 0.044 |
| 429 | 0.045 | 413 | 0.012 | 289 | 0.014 |
| 501 | 0.041 | | | 364 | 0.013 |

[a] In the range 260–600 nm with $f > 0.01$.

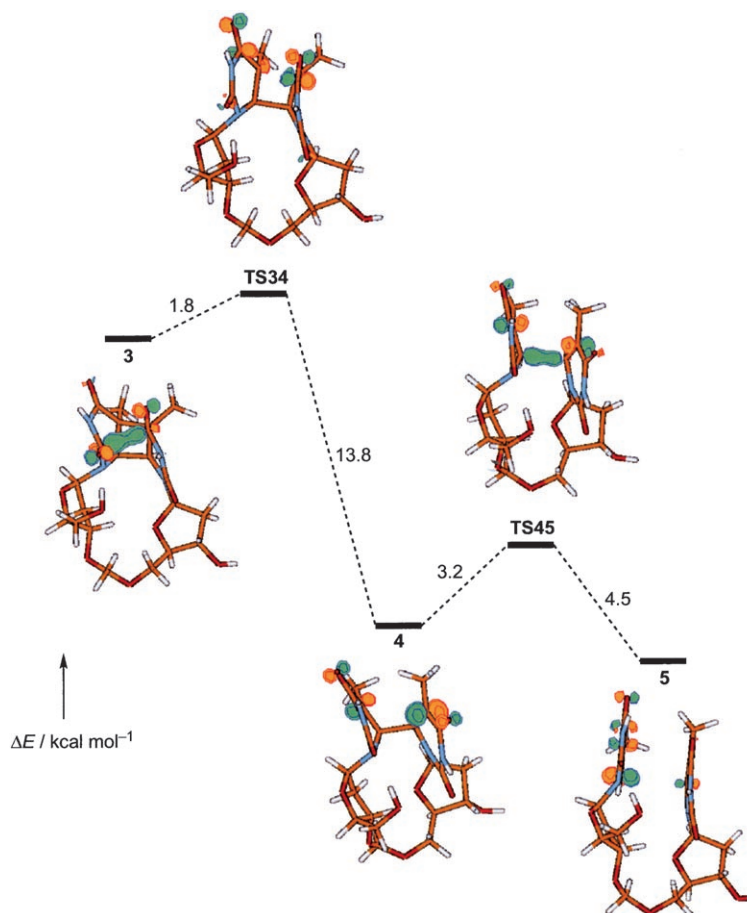


Figure 2. Relative energies ΔE and SOMO of the radical anion species at the stationary points along the reaction pathway **3**→**4**→**5** computed at the B1B95/6-31+G** level.

Figure 2 shows the energy profile of the transformation from **3** to **5** and the SOMO of the radical anion species at the stationary points along the reaction pathway computed at the B1B95/6-31+G** level. In Table 2, the detailed spin density distributions are reported. The unpaired electron in the radical anion **3** is mainly localized at the C2–O2 and C4'–O4' carbonyl groups (that is, on both thymine rings), the SOMO being stabilized by the through space in-phase interaction of the π -antibonding (π_{CO}^*) orbitals of the two carbonyl groups (C2...C4' distance is as short as 2.326 Å). The energy barrier, corrected for the zero-point vibrational

Table 2. Spin density at the heavy atoms of the thymine bases at the stationary points along the reaction pathway leading from the dimer radical anion **3** to the monomer radical anion **5** computed at the B1B95/6-31+G** level.

| Atom | 3 | TS34 | 4 | TS45 | 5 |
|------|----------|-------|----------|-------|----------|
| N1 | 0.01 | 0.03 | 0.02 | 0.00 | -0.03 |
| C2 | 0.24 | 0.11 | 0.00 | 0.01 | 0.01 |
| O2 | 0.18 | 0.04 | -0.01 | -0.01 | -0.01 |
| N3 | -0.05 | -0.07 | 0.04 | 0.03 | 0.03 |
| C4 | 0.02 | 0.13 | -0.01 | 0.04 | 0.11 |
| O4 | 0.04 | 0.16 | 0.05 | 0.08 | 0.08 |
| C5 | -0.04 | 0.03 | 0.26 | 0.23 | -0.05 |
| C6 | 0.01 | 0.01 | 0.03 | 0.10 | 0.51 |
| N1' | -0.01 | 0.01 | 0.02 | 0.03 | -0.01 |
| C2' | 0.03 | 0.04 | 0.00 | 0.01 | 0.01 |
| O2' | 0.02 | 0.04 | 0.00 | -0.01 | 0.00 |
| N3' | -0.01 | -0.02 | 0.03 | 0.03 | 0.03 |
| C4' | 0.20 | 0.21 | -0.01 | 0.04 | 0.06 |
| O4' | 0.18 | 0.13 | 0.12 | 0.07 | 0.02 |
| C5' | 0.02 | 0.14 | 0.43 | 0.27 | -0.06 |
| C6' | 0.04 | 0.03 | -0.07 | 0.02 | 0.31 |

energy (ZPVE), for the C5–C5' cleavage is only 1.8 kcal mol⁻¹ (see transition-state TS34). This bond break is 12.0 kcal mol⁻¹ exothermic and partially ionic, as the unpaired electron in **4** remains mainly localized at C5'. A rotation of about 40° around the C6–C6' bond is observed. In TS34, the stabilizing interaction between the π_{CO}^* orbitals of the C2–O2 and C4'–O4' groups strongly decreases due to a decrease of the overlap between the π_{CO}^* orbitals of the two interacting groups and the $\pi_{\text{C4-O4}}^*$ orbital becomes more stable than the π_{CO}^* orbitals of the other carbonyl groups. This produces a shift of spin density in TS34 from C2–O2 to C4–O4 and a partially ionic break of the C5–C5' bond with electron transfer to the O4 atom. Indeed, the unpaired electron both in TS34 and in **4** is more localized at C5' than at C5. The subsequent break of this C–C bond (see TS45) is computed to occur with a slightly higher energy barrier (3.2 kcal mol⁻¹). This process is 1.3 kcal mol⁻¹ exothermic.^[14] The unpaired electron in **5** is localized mainly at the C6 atom. However, the SOMO is weakly stabilized by the through-space interaction with the C6' orbitals, the C6...C6' distance being relatively small (3.136 Å).

In DNA duplex, form **5** should be further favored due to π -stacking interactions, indicating that the unpaired electron on the (A·T)⁻ pair should interact with the adjacent A·T pair. Assuming a “normal” pre-exponential factor (that is, $\log A/s^{-1} = 13$),^[15] we estimated that the half-life for the decay of the radical anion **3** is only 1–2 ps, whereas the half-life for the decay of the radical anion **4** is 15–16 ps, both at room temperature.

Product studies from γ -radiolysis: Continuous radiolysis was also performed by using two ⁶⁰Co-sources with different dose rates (approximately, 0.6 or 10 Gy min⁻¹). In a typical experiment, 5 mL aqueous solutions containing 0.3–3.0 mM T<>T dimer **2** and 0.25 M *i*PrOH at natural pH were vacuum-deoxygenated. Then the required dose was applied and the crude reaction mixture was analyzed by HPLC and

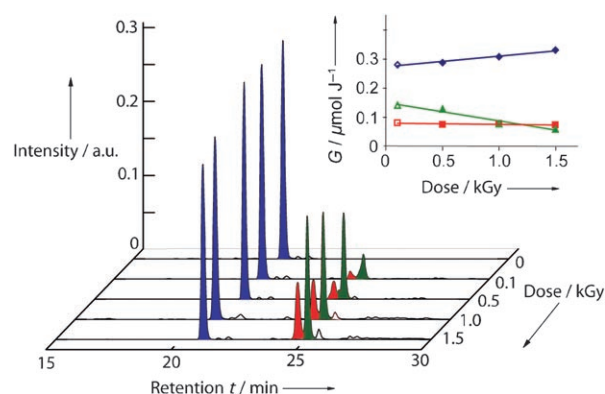
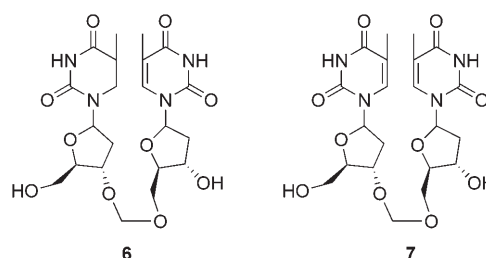


Figure 3. Irradiation of T<>T dimer **2** (3.0 mM) in the presence of 0.25 M *i*PrOH at a dose rate of ≈ 0.6 Gy min⁻¹ (0.1 kGy) or ≈ 10 Gy min⁻¹ (0.5, 1.0, and 1.5 kGy). The HPLC peaks of the T<>T dimer **2** are highlighted in blue, while the peaks for the products **6** and **7** are highlighted in red and green, respectively. The inset shows the chemical radiation yields (G) for the consumption of **2** (blue) and the production of **6** (red) and **7** (green) as a function of the irradiation dose.

LCMS. Figure 3 shows the HPLC analyses at different doses, in case of the experiment with the highest dimer concentration used. However, the same results were obtained regardless of the substrate concentration and dose rate. The disappearance of starting material (blue peaks) is accompanied by the appearance of two new major products, which were identified as **6** (red peaks) and **7** (green peaks). The inset of Figure 3 shows the analysis of the data in terms of radiation chemical yields (G , $\mu\text{mol J}^{-1}$). The disappearance of the T<>T dimer **2**, $G(-\mathbf{2})$, extrapolated at zero dose was calculated to be $0.27 \mu\text{mol J}^{-1}$ which corresponds to $G(e_{\text{aq}}^-)$, whereas $G(\mathbf{6}) = 0.08$ and $G(\mathbf{7}) = 0.015 \mu\text{mol J}^{-1}$ represent the 85% yield of the reaction products. When the reaction was carried out in D₂O, product **6** contained two deuterium atoms. We suggest that once the radical anion **5** is formed, it is first protonated^[12b,16] followed by slow tautomerization which leads to the incorporation of the first deuterium atom at C5. Then a radical–radical disproportionation may occur with either itself or with the Me₂C(·)OD radical [Eq. (3)]. This would lead to the incorporation of a second deuterium atom at C(6).



Our results do not support the finding that the one-electron reduction of **1a** and the subsequent cleavage of the cyclobutane ring proceeds by means of a radical chain mechanism, due to the transfer of an electron from the monomer radical anion (analogous to **5**) to another dimer molecule of **1a**.^[9] If such a mechanism would be involved then the

$G(-2)$ would be expected to be higher than $0.27 \mu\text{molJ}^{-1}$, implying that a single electron cleaves several cyclobutane rings. Our experiments involving a high substrate concentration (3.0 mM) and a low dose rate (0.6 Gymin^{-1}), which ensures low radical concentration and favorable conditions for a radical chain reaction, show that radical disproportionation reactions govern the reaction outcome, including formation of the product **7**. Although in our model reaction, $\text{T}^{\cdot-}$ is unable to transfer an electron to the $\text{T} \langle \rangle \text{T}$ dimer **2**, this reaction may occur inside a DNA duplex due to altered redox potentials in the π -stack.^[17]

Conclusion

The reaction of hydrated electrons with the $\text{T} \langle \rangle \text{T}$ dimer **2** is a diffusion-controlled process and the resulting radical anion **3**, in which the spin density and charge distribution are located in both thymine rings, undergoes a fast splitting of the cyclobutane ring by two successive C–C bond cleavages. The estimated half-life of a few ps is in accord with the recent direct observation of the thymine dimer repair in DNA by photolyase.^[2b] Hence, DNA photolyases do not accelerate the cleavage process which suggests that the photolyase-catalyzed repair process is fully entropy driven. The enthalpic stabilization of the transition state seems to be a very minor component in the catalytic reaction.

Experimental Section

Materials: Compound **2** was prepared following a known procedure.^[18] The solutions of nucleosides were freshly prepared immediately before each experiment.

Pulse radiolysis: The experiments were performed on the picosecond electron accelerator ELYSE (University Paris-sud, Orsay).^[19] Electron pulses at 9 MeV energy and 10 ps duration have been applied to the thymine dimer solution. The dose deposited in water was around 20 Gy (that is, $1.2 \times 10^{-5} \text{ M}$ of hydrated electrons) in the irradiated volume under the standard experimental conditions. Due to the 2 to 5 mm diameter of the electron beam, the irradiated volume is less than 0.25 mL. A stock solution of 100 mL containing 3.4 mM substrate and 0.3 M *t*BuOH at pH 8.9 (phosphate buffer 10 mM) in deionized water has been used, which circulates in the $10 \times 5 \text{ mm}$ fused silica irradiation cell at a flow rate of 30 mLmin^{-1} by means of a peristaltic pump. As the electron pulses were applied at a frequency of 1 Hz, the solution was renewed between each pulse thus resulting in a total of 200 pulses applied to the 100 mL solution.

Absorption detection was performed by using the white light beam of a special home made Xenon flash lamp focused through the cell colinearly with electron beam. The path length was 10 mm. The light was then focused on the entrance slit of a flat field spectrograph, which dispersed the light on the entrance optics of a streak-camera (model C-7700 from Hamamatsu).^[20]

Two series of 200 pulses have been applied to get two absorption measurements on a full time scale of 500 ns. The first one was done in order to record simultaneously the absorption from 280 to 420 nm and the second one from 370 to 670 nm. In each case, the 200 images provided by the streak-camera were averaged in a unique image used for the calculation of the optical density, by reference to the similar image obtained on the averaging of 200 flashes of the analyzing light alone elsewhere. Full

details on this new detection system will be published. All the kinetic data and the absorption spectra were obtained from these two series.

Continuous radiolysis: The experiments were performed at room temperature ($22 \pm 2^\circ\text{C}$) by using 5 mL samples with ^{60}Co -Gammacells, with a dose rate of approximately 10 Gymin^{-1} or approximately 0.6 Gymin^{-1} . The absorbed radiation dose was determined with the Fricke chemical dosimeter, by taking $G(\text{Fe}^{3+}) = 1.61 \mu\text{molJ}^{-1}$.^[21] Reaction mixtures were analyzed with a Zorbax SB-C18 column ($4.6 \times 150 \text{ mm}$), eluted in triethylammonium acetate buffer (20 mM, pH 7) with a 0–25% acetonitrile linear gradient over 30 min with a flow rate of 1.0 mLmin^{-1} (detection at 250 nm). Products were identified by LCMS analysis.

Computational details: Hybrid meta DFT calculations with the B1B95 (Becke88^[22]-Becke95^[23] model for thermochemistry) functional^[24] were carried out by using the Gaussian 03 system of programs.^[25] This HMDFT method was found to give a good performance for thermochemistry^[24,26] and electron affinities (EA).^[26b] An unrestricted wavefunction was used for radical species. Total energies were obtained by employing the valence double- ζ basis set supplemented with polarization functions.^[27] Addition of standard diffuse functions on heavy atoms^[28] to better describe the anion states were found to give reliable results, although the radical anion **3** is computed to be kinetically slightly unstable in the gas phase, the vertical EA of **2** being slightly negative (VEA = -0.17 eV). However, the adiabatic EA of **2** is computed to be largely positive (AEA = 0.94 eV) and the distribution of the unpaired electron in the valence atomic orbitals of the SOMO at any stationary point of the energy surface (that is, minima and transition states) satisfies the outlined criterions.^[29] Hence the B1B95 calculations were carried out by using the 6-31+G** basis set. Total energies were corrected for the zero-point vibrational energy (ZPVE) computed from frequency calculations by using a scaling factor of 0.9735 to account for anharmonicity.^[26a] The nature of the ground (zero imaginary frequency) and transition (one imaginary frequency) states was verified by frequency calculations. Time-dependent (TD)B3LYP method employing a triple- ζ basis set (TD-B3LYP/6-311G**//B1B95/6-31+G**) was used to compute optical spectra of the radical anions **3–5**.^[13]

Acknowledgements

Work supported in part by the Volkswagen Foundation and the Marie Curie Research Training Network of the European Community MRTN-CT-2003–505086 [CLUSTOXDNA].

- [1] a) D. E. Brash, *Trends Genet.* **1997**, *13*, 410; b) S. Kozmin, G. Slezak, A. Reynaud-Angelin, C. Elie, Y. de Rycke, S. Boiteux, E. Sage, *Proc. Natl. Acad. Sci. USA* **2005**, *102*, 13538; c) S. Mouret, C. Baudouin, C. Charveron, A. Favier, J. Cadet, T. Douki, *Proc. Natl. Acad. Sci. USA* **2006**, *103*, 13765; d) W. j. Schreier, T. E. Schrader, F. O. Koller, P. Gilch, C. E. Crespo-Hernández, V. N. Swaminathan, T. Carell, W. Zinth, B. Kohler, *Science* **2007**, *315*, 625.
- [2] a) A. Sancar, *Chem. Rev.* **2003**, *103*, 2203; b) Y.-T. Kao, C. Saxena, L. Wang, A. Sancar, D. Zhong, *Proc. Natl. Acad. Sci. USA* **2005**, *102*, 16128.
- [3] F. Boussicault, O. Krüger, M. Robert, U. Wille, *Org. Biomol. Chem.* **2004**, *2*, 2742.
- [4] S.-R. Yeh, D. E. Falvey, *J. Am. Chem. Soc.* **1991**, *113*, 8557.
- [5] A. Pezeshk, I. D. Podmore, P. F. Heelis, M. C. R. Symons, *J. Phys. Chem.* **1996**, *100*, 19714.
- [6] P. F. Heelis, D. J. Deeble, S.-T. Kim, A. Sancar, *Int. J. Radiat. Biol.* **1992**, *62*, 137.
- [7] M. P. Scannell, G. Prakash, D. E. Falvey, *J. Phys. Chem. A* **1997**, *101*, 4332.
- [8] H.-A. Wagenknecht, *Nat. Prod. Rep.* **2006**, *23*, 973.
- [9] a) T. Carell, C. Behrens, J. Gierlich, *Org. Biomol. Chem.* **2003**, *1*, 2221; b) C. Behrens, M. K. Cichon, F. Grolle, U. Hennecke, T. Carell, *Top. Curr. Chem.* **2004**, *236*, 187.

- [10] a) B. Giese, B. Carl, T. Carl, T. Carell, C. Behrens, U. Hennecke, O. Schiemann, E. Feresin, *Angew. Chem.* **2004**, *116*, 1884; *Angew. Chem. Int. Ed.* **2004**, *43*, 1848; b) C. Haas, K. Kräling, M. Cichon, N. Rahe, T. Carell, *Angew. Chem.* **2004**, *116*, 1878; *Angew. Chem. Int. Ed.* **2004**, *43*, 1842.
- [11] a) G. V. Buxton, C. L. Greenstock, W. P. Helman, A. B. Ross, *J. Phys. Chem. Ref. Data* **1988**, *17*, 513; b) L. Wojnárovits, E. Takács, K. Dajka, S. S. Emmi, M. Russo, M. D'Angelantonio, *Radiat. Phys. Chem.* **2004**, *69*, 217.
- [12] a) S. Steenken, J. P. Telo, H. M. Novais, L. P. Candeias, *J. Am. Chem. Soc.* **1992**, *114*, 4701; b) A pK_a value of 6.9 is reported for the protonated electron adduct of thymidine.^[12a]
- [13] TD-DFT calculations were found by us to provide reliable optical transitions in nucleosides see: a) C. Chatgililoglu, C. Ferreri, R. Bazzanini, M. Guerra, S.-Y. Choi, C. J. Emanuel, J. H. Horner, M. Newcomb, *J. Am. Chem. Soc.* **2000**, *122*, 9525; b) C. Chatgililoglu, M. Guerra, Q. G. Mulazzani, *J. Am. Chem. Soc.* **2003**, *125*, 3839; c) C. Chatgililoglu, C. Caminal, A. Altieri, Q. G. Mulazzani, G. C. Vougioukalakis, T. Gimisis, M. Guerra, *J. Am. Chem. Soc.* **2006**, *128*, 13796.
- [14] Protonation of radical anion **4** should be a slower process at pH 7. Moreover, the energy barrier computed without ZPVE for C6–C6' cleavage in the **4**(+H⁺) is computed to be 6.7 kcal mol⁻¹ higher than in **45**.
- [15] S. W. Benson, *Thermochemical Kinetics*, 2nd ed., Wiley, New York, **1976**.
- [16] Radiolysis of neutral water also leads to H⁺ (0.34 μmol J⁻¹) besides the species shown in Equation (1). The solution after the irradiation dose of 1 kGy gave pH ≈ 6.
- [17] J. Gu, Y. Xie, H. F. Schaefer, *J. Phys. Chem. B* **2005**, *109*, 13067.
- [18] J. Butenandt, A. P. M. Eker, T. Carell, *Chem. Eur. J.* **1998**, *4*, 642.
- [19] J. Belloni, H. Monard, F. Gobert, J. P. Larbre, A. Demarque, V. De Waele, I. Lampre, J. L. Marignier, M. Mostafavi, J. C. Bourdon, M. Bernard, H. Borie, T. Garvey, B. Jacquemard, B. Leblond, P. Lepercq, M. Omeich, M. Roch, J. Rodier, R. Roux, *Nucl. Instrum. Methods Phys. Res. Sect. A* **2005**, *539*, 527.
- [20] J. L. Marignier, V. de Waele, H. Monard, F. Gobert, J. P. Larbre, A. Demarque, M. Mostafavi, J. Belloni, *Radiat. Phys. Chem.* **2006**, *75*, 1024.
- [21] J. W. T. Spinks, R. J. Woods, *An Introduction to Radiation Chemistry*, 3rd ed., Wiley, New York, **1990**, p. 100.
- [22] A. D. Becke, *Phys. Rev. A* **1988**, *38*, 3098.
- [23] A. D. Becke, *J. Chem. Phys.* **1996**, *104*, 1040.
- [24] Y. Zhao, B. J. Lynch, D. G. Truhlar, *Chem. Phys. Chem. Phys.* **2004**, *6*, 673.
- [25] Gaussian 03, Revision B.5, M. J. Frisch, G. W. Trucks, H. B. Schlegel, G. E. Scuseria, M. A. Robb, J. R. Cheeseman, J. A. Montgomery, Jr., T. Vreven, K. N. Kudin, J. C. Burant, J. M. Millam, S. S. Iyengar, J. Tomasi, V. Barone, B. Mennucci, M. Cossi, G. Scalmani, N. Rega, G. A. Petersson, H. Nakatsuji, M. Hada, M. Ehara, K. Toyota, R. Fukuda, J. Hasegawa, M. Ishida, T. Nakajima, Y. Honda, O. Kitao, H. Nakai, M. Klene, X. Li, J. E. Knox, H. P. Hratchian, J. B. Cross, C. Adamo, J. Jaramillo, R. Gomperts, R. E. Stratmann, O. Yazyev, A. J. Austin, R. Cammi, C. Pomelli, J. W. Ochterski, P. Y. Ayala, K. Morokuma, G. A. Voth, P. Salvador, J. J. Dannenberg, V. G. Zakrzewski, S. Dapprich, A. D. Daniels, M. C. Strain, O. Farkas, D. K. Malick, A. D. Rabuck, K. Raghavachari, J. B. Foresman, J. V. Ortiz, Q. Cui, A. G. Baboul, S. Clifford, J. Cioslowski, B. B. Stefanov, G. Liu, A. Liashenko, P. Piskorz, I. Komaromi, R. L. Martin, D. J. Fox, T. Keith, M. A. Al-Laham, C. Y. Peng, A. Nanayakkara, M. Challacombe, P. M. W. Gill, B. Johnson, W. Chen, M. W. Wong, C. Gonzalez, and J. A. Pople, Gaussian, Inc., Pittsburgh PA, **2003**.
- [26] a) Y. Zhao, B. J. Lynch, D. G. Truhlar, *J. Phys. Chem. A* **2004**, *108*, 2715; b) Y. Zhao, D. G. Truhlar, *J. Phys. Chem. A* **2004**, *108*, 6908.
- [27] a) P. C. Hariharan, J. A. Pople, *Theor. Chim. Acta* **1973**, *28*, 213; b) M. M. Francl, W. J. Pietro, W. J. Hehre, J. S. Binkley, M. S. Gordon, D. J. De Frees, J. A. Pople, *J. Chem. Phys.* **1982**, *77*, 3654.
- [28] T. Clark, J. Chandrasekhar, P. v. R. Schleyer, *J. Comput. Chem.* **1983**, *4*, 294.
- [29] M. Guerra, *J. Phys. Chem. A* **1999**, *103*, 5983.

Received: May 27, 2007
Published online: August 10, 2007